Noise Suppression in Eddy Current C-Scan Images Using a Non-linear Adaptive Maximum Likelihood Filter

R. P.R. Hasanzadeh[i], S.H.H. Sadeghi[ii], A.H. Rezaie[iii], A.R. Moghaddamjoo[iv], M. Ahmadi[v]

ABSTRACT

In this paper, a non-linear local adaptive Maximum Likelihood filter is proposed for analyzing EC C-scan images. The model of EC noise in this filter is assumed to be non-zero mean complex Gaussian process. By introducing an enhancing factor, we show that a better sharpening of the boundary and details of defects are achievedwhile the effect of noise on the defect reconstruction is reduced. Theoretical and experimental results are presented to confirm the performance of the proposed filter.

KEYWORDS

Eddy Current, Additive Complex Gaussian noise, Adaptive, Maximum Likelihood.

1. INTRODUCTION

Nondestructive evaluation (NDE) includes a wide range of inspection methods such as visual, radiography, ultrasonic and electromagnetic with several applications in the field of medical and industry [1]. The eddy current (EC) technique is the most commonly used nondestructive testing (NDT) method for detection and sizing of defects in conductive materials. This method works as a result of the interaction between an ac current-carrying probe (coil) and the material under the test [1]. This interaction appears as an impedance variation of the probe which is due to the variations of density, permeability and conductivity of the material [2].

A visual observation technique, based on C-scan imaging, is often used for analysis of eddy current test data [3]. It is desirable that the true defect signals in EC C-scan images have sufficiently large amplitudes in comparison with the noise [2]. One solution for noise reduction is based on utilizing a statistical model that characterizes the probability density function of noise in the EC C-scan images. The statistical model used for noise process in ultrasonic images is the multiplicative Rayleigh speckle [4] whereas in magnetic resonance imaging data, an additive Rician [5] model is found to be appropriate. The model of noise associated with the EC signal is generally taken to be additive, uncorrelated and complex Gaussian (CG) with zero mean and comparable variance for each quadrature channel [2]. Also, the straight model of noise for signal amplitude (absolute of impedance) changes to Rician distribution [5].

The non-stationary nature of images in addition to the limitations of linear spatial filtering have motivated many researchers towards the investigation of filters which adjust their smoothing properties at each point of the image according to the local image content [6, 7]. Therefore, non-linear methods are successful alternatives to linear methods for image processing because these

i PhD from Electrical Engineering Department, Amirkabir University of Technology, Currently is Assistant Professor with Electrical Engineering Department, Guilan University, P.O. Box 41635-13769, Rasht, IRAN, e-mail: hasanzadehpak@guilan.ac.ir.

ii Professor, Electromagnetic Research Laboratory, Electrical Engineering Department, Amirkabir University of Technology, Tehran, 15914, IRAN, e-mail: sadeghi@aut.ac.ir.

iii Assistant Professor, Automation Research Laboratory, Electrical Engineering Department Amirkabir University of Technology, Tehran, 15914, IRAN, e-mail: rezaie@aut.ac.ir

iv Professor, Department of Electrical Engineering and Computer Science, University of Wisconsin-Milwaukee, P.O. Box 784, Milwaukee, WI 53201-0784, USA, e-mail: reza@uwm.edu.

v Assistant Professor, NDT Research Laboratory, Mechanical Engineering Department Amirkabir University of Technology, Tehran, 15914, IRAN, e-mail: ahmadin@aut.ac.ir.

techniques can locally provide a dynamic structure for the best estimation of noise-defect transition [7]. The experimental results indicate that the first processing levels of human visual system (HVS) possess nonlinear characteristics for better estimation of objects [7, 8].

Because of inhomogeneous micro-structure of defects and noise, it is difficult to extract both boundary and size of the defect. Linear techniques do not provide good results for noise-defect separation as both the noise structure and defect signals in C-scan images have the same intensities. Therefore, non-linear techniques such as the adaptive maximum likelihood (AML) filter are good alternatives for defect enhancement [8, 9].

Linear noise elimination methods such as spatial averaging and Wiener filter have been used in signal processing [11]. However, these methods suffer from some limitations due to their low pass property which causes image degradation through suppression of edges and small details [9]. Images are in general non-stationary signals and as such perform poorly under linear modeling and linear filtering techniques [11].

Several classes of nonlinear filters exist. They include homomorphic, nonlinear mean, nonlinear partial differential equation, morphological, order statistics, polynomial and fuzzy filters [9].

In this paper, we first make use of the AML filter for separating noise and defect in an EC inspection process which is discussed in section 2. In Section 3, the design of the AML filter that deals with lift-off noise removal on EC C-Scan images is formulated. In this case, noise is modeled as a non-zero mean CG. Also in this section, the modification of the AML filter is described by introducing an enhancing factor (α). In Section 4, the development of an edge detection enhancement operator for better estimation of the defects boundary is described. It can help improve image understanding in EC practices. In Section 5, simulated and experimental results are presented to examine the performance of the proposed filter.

2. THE AML FILTER

The AML filter is one class of non-linear mean filters used for noise suppression. It works with local image adaptation based on moving window. The result of local windows is enhanced for the best noise removal based on pre-defined probability density function of noise [12]. In this section we develop this filter to process of EC C-scan images.

A. Filter Model

Consider an image x consisting of two parts: a low-frequency part x_L and a high-frequency part x_H as $x = x_L + x_H$ [13]. The low-frequency component depends on the homogeneous regions of image while the high-frequency component depends on the near edge regions. The maximum likelihood (ML) estimation denoted by $\hat{s}_{ML}(k,l)$ is obtained based on the observations in a moving window W centered at the current pixel (k, l). The ML estimation is proposed as the low-frequency component [8]. Thus the estimate of the original signal at (k, l), is as follows.

$$\hat{s}(k,l) = \hat{s}_{ML}(k,l) + \beta(k,l).[x(k,l) - \hat{s}_{ML}(k,l)] \quad (1)$$

where $x(k, l)$ is the noisy observation at pixel (k, l), $\hat{s}_{ML}(k,l)$ is the maximum likelihood estimate of $s(k, l)$ based on the observations $x(k-i, l-j) \in W$, $\beta(k,l)$ is a weighting factor, approximating the local signal-to-noise ratio (SNR) over the window W, and $\hat{s}(k,l)$ is the signal-adaptive filter output at pixel (k, l). For simplicity we eliminate index (k, l) in exhibition of formulas.

By selecting β near to 1, the result of (1) becomes equal to the original noisy image and when it is near to 0, the high-frequency component is suppressed and the maximum noise reduction is occurred. The value of β can be derived for the best approximation of the original (noiseless) signal.

B. Signal Dependent Weighting Factor

A local mean squared error (MSE), e, can be used as a criterion to best approximate the noiseless signal, s from its estimation, $\hat{s}$ obtained from (1).

$$e = E_W[(s-\hat{s})^2] = E_W[(s-\hat{s}_{ML})^2] + \beta^2 E_W[(x-\hat{s}_{ML})^2] - 2\beta E_W[(s-\hat{s}_{ML})(x-\hat{s}_{ML})] \quad (2)$$

where the local expectation value $E_W[.]$ and β are calculated over a window W centered at pixel (k, l).

Minimizing e relative to β by differentiating (2) with respect to β and setting the result equal to zero yields:

$$\beta = \frac{E_W[(s-\hat{s}_{ML})(x-\hat{s}_{ML})]}{E_W[(x-\hat{s}_{ML})^2]} \quad (3)$$

The weighting factor (3) is a general form and can be obtained for non-zero mean Gaussian. By replacing (3) in (2), the error function can be obtained as:

$$e = E_W[(s-\hat{s})^2] = E_W[(s-\hat{s}_{ML})^2] - \beta^2 E_W[(x-\hat{s}_{ML})^2] \quad (4)$$

3. PROCESSING NOISY EC IMAGES

An EC image enhancement is often performed by suppression of noise [16, 17]. Noise may be caused by variation of the probe lift-off and drift, or other unwanted signals such as porosity in the test specimen [16, 17]. In this section, first, we derive the value of the weighting factor and $\hat{s}_{ML}$ based on ML criterion. Then (1) is modified for enhancing the defect details.

A. Complex Gaussian Model of Noise

Since EC images are obtained from complex probe impedance data, x, the formation of a model for EC signals can be achieved as [2],

$$x = s + n = x_r + jx_i = s_r + n_r + j(s_i + n_i) \quad (5)$$

where s is the true signal, n denotes the measurement noise and unwanted signals such as probe lift-off from the specimen under the test [14]. It is noted that s, n and x contain real (r) and imaginary (i) parts As shown in (5), real and imaginary parts are statistically independent and can be obtained separately from each other [15].

Noise model in the EC technique is usually modeled as an additive zero-mean complex Gaussian which is assumed to be independent of the signal [2]. Probe lift-off is an inevitable part of EC inspection. It occurs when a gap exists between the probe and the material under evaluation [14]. The spatial variation of the probe enforces an unwanted effect on the original signal that is taken usually into account by changing the noise model to a nonzero-mean complex Gaussian process as:

$$f_n(n) = \frac{1}{\sqrt{2\pi}\sigma_n} \exp\left[-\frac{(n-\mu)^2}{2\sigma_n^2}\right] \quad (6)$$

where σ_n and μ are, respectively, variance and mean of noise.

The conditional density function of a complex observation x assuming s is given by

$$f_{x|s}(X \mid S) = \frac{1}{\sqrt{2\pi}\sigma_n} \exp\left[-\frac{(X-S-\mu)^2}{2\sigma_n^2}\right] \quad (7)$$

For N complex observations $x^1, x^2, ..., x^N$, the conditional probability distribution function (pdf) of the observations assuming s can be estimated as follows,

$$f_{x|s}(X \mid S) = \prod_{i=1}^{N} f_{x_i|s}(X_i \mid S) = \left(\frac{1}{\sigma_n\sqrt{2\pi}}\right)^N \exp\left[-\frac{1}{2\sigma_n^2}\sum_{i=1}^{N}(X_i - S - \mu)^2\right] \quad (8)$$

The N observations are obtained from the measurements in the moving window W centered at the pixel whose value s is to be estimated. We assume that s and n are statistically independent. The ML estimation of s, by maximizing the log-likelihood of (8) is given by

$$\hat{s}_{ML} = \frac{1}{N}\sum_{i=1}^{N} X_i - \mu \quad (9)$$

Using (5)-(9), it can be shown that

$$E(s) = E(x) - \mu = \hat{S}_{ML} \quad (10\text{-a})$$

$$E(xs) = E(x^2) - \mu E(s) - \sigma_n^2 - \mu^2 \quad (10\text{-b})$$

$$E(s^2) = E(x^2) - 2\mu\hat{s}_{ML} - \sigma_n^2 - \mu^2 \quad (10\text{-c})$$

From (10), the following equality can be derived.

$$\begin{aligned} &\textit{Define}: && \sigma_{xs}^2 = E[xs] - \hat{s}_{ML}.E[x] \\ &\textit{Define}: && \sigma_s^2 = E[s^2] - \hat{s}_{ML}{}^2 \\ &\textit{Define}: && \sigma_x^2 = E[(x - E[x])^2] = E[x^2] - E^2(x) \\ &\textit{then} && \sigma_{xs}^2 = \sigma_s^2 = \sigma_x^2 - \sigma_n^2 \end{aligned} \quad (11)$$

Using (3), the value of the weighting factor β for CG noise model can be obtained as follows:

$$\beta = \frac{(\sigma_x^2 - \sigma_n^2)}{\sigma_x^2 + \mu^2} = 1 - \left(\frac{\sigma_n^2 + \mu^2}{\sigma_x^2 + \mu^2}\right) \quad (12)$$

By replacing (12) in (4), the mean square error (MSE) is given by

$$e = (\sigma_x^2 - \sigma_n^2).\left(\frac{\sigma_n^2 + \mu^2}{\sigma_x^2 + \mu^2}\right) = (\sigma_n^2 + \mu^2).\beta \quad (13)$$

where it is seen that the error function in (8) is valid only for $\sigma_x \geq \sigma_n$. Therefore, this method cannot be used for $\sigma_x < \sigma_n$ [18]. For $\sigma_x < \sigma_n$, the best approximate can be obtained from ML estimation. Equations (13) is modified by *sign* operator to eliminate artifacts produced by the negative value of difference variances as:

$$\beta = \begin{cases} 1 - \left(\frac{\sigma_n^2 + \mu^2}{\sigma_x^2 + \mu^2}\right) & \sigma_x \geq \sigma_n \\ 0 & \sigma_x < \sigma_n \end{cases} \quad (14)$$

B. Modified SAML

Referring to (13) and (14), it is seen that the probe lift-off is an effective parameter on the quality of defect detection. Although (3) is obtained for minimum error, one should be careful that it may cause elimination of high frequency details of a defect (second term of (1)). The objective is thus to find the value of β such that it provides the best detection of defect details while minimizing the error (noise). This is done by introducing an enhancing factor in the second term of (1) as follows:

$$\hat{s} = \hat{s}_{ML} + \beta(\alpha).[x - \alpha\hat{s}_{ML}] \quad (15)$$

The error function (8) changes to:

$$\begin{aligned} e &= E_W[(s - \hat{s})^2] = E_W[(s - \hat{s}_{ML})^2] + \\ &\beta(\alpha)^2 E_W[(x - \alpha.\hat{s}_{ML})^2] - 2\beta(\alpha)E_W[(s - \hat{s}_{ML})(x - \alpha.\hat{s}_{ML})] \end{aligned} \quad (16)$$

To minimize the error relative to β, we differentiate (20) with respect to β and set the result equal to zero. This leads to

$$\beta(\alpha) = \frac{E_W[(x - \alpha.\hat{s}_{ML})(s - \hat{s}_{ML})]}{E_W[(x - \alpha.\hat{s}_{ML}))^2]} \quad (17)$$

By replacing the statistical values of additive CG noise, the result of the weighting factor and error function can be obtained as follows.

$$\beta(\alpha) = 1 - \frac{(\sigma_n^2 + [\mu - (\alpha - 1).\hat{s}_{ML}]^2)}{E[(x - \alpha.\hat{s}_{ML})^2]} = \frac{\sigma_x^2 - \sigma_n^2}{\sigma_x^2 + [\mu - (\alpha - 1).\hat{s}_{ML}]^2} \quad (18)$$

$$\begin{aligned} e(\alpha) &= E_W[(s - \hat{s}_{ML})^2] - \beta(\alpha)^2 E_W[(x - \alpha.\hat{s}_{ML})^2] \\ &= (\sigma_x^2 - \sigma_n^2).\left(\frac{\sigma_n^2 + [\mu - (\alpha - 1).\hat{s}_{ML}]^2}{\sigma_x^2 + [\mu - (\alpha - 1).\hat{s}_{ML}]^2}\right) \end{aligned} \quad (19)$$

It can be shown that the maximum value of β in (18) and the minimum value of error function in (19) can be obtained by the following value of the enhancing factor, α.

$$\alpha = 1 + (\mu / \hat{s}_{ML}) = E_W[x] / \hat{s}_{ML} \quad (20)$$

From (20), the best estimate of the original signal, weighting factor for maximum details β_{max} and error

function for minimum error $e_{\min}$ can be obtained as follows,

$$\hat{s} = \hat{s}_{ML} + \beta_{\max}.(x - E[x]) = (1 - \beta_{\max}).\hat{s}_{ML} + \beta_{\max}.[x - \mu] \quad (21)$$

$$\beta_{\max} = \begin{cases} 1 - (\frac{\sigma_n^2}{\sigma_x^2}) & \sigma_x \geq \sigma_n \\ 0 & \sigma_x < \sigma_n \end{cases} \quad (22)$$

$$e_{\min} = \sigma_n^2.(1 - (\frac{\sigma_n}{\sigma_x})^2) = \sigma_n^2.\beta_{\max} \quad (23)$$

C. Numerical Comparison

It is important to examine the ability of the proposed algorithm in the presence of various SNRs. One definition of SNR is the ratio of the two variances of n and x [11]. Fig (1) shows variations of the weighting factor in (18) for several values of the enhancing factor defined in (20). Equation (21) is the best estimation of $\hat{s}$ with the minimum suppression of details of the original signal. It can be seen that the value of $\beta_{\max}$ in (22) directly affects the high frequency details of the original signal in (21).

Referring to Fig (1), it can be seen that for $\sigma_x >> \sigma_n$, the value of β is less dependent on the value of α. However, for comparable values of the two variances, the AML technique may eliminate the details of a defect while suppressing noise. Thus, the value of α becomes important for detection of the details of an image, indicating that $\alpha=1$ is not considered as the best approximation. On the other hand, the ratio result of error functions (13) and (23), given below,

$$\frac{e_{\min}}{e} = \frac{\sigma_n^2.\beta_{\max}}{(\sigma_n^2 + \mu^2).\beta} = \frac{1 - \beta_{\max}}{1 - \beta} \leq 1 \quad (24)$$

shows that the minimum error is obtained in the case of the modified AML (MAML) method.

It is worth noting that the results are given for $\sigma_x \geq \sigma_n$. Otherwise, both the AML/MAML methods lead to ML estimation. Table (1) shows the general form, AML and MAML filters with their corresponding weighting factors.

4. Boundary Detection of a Defect

Referring to (19) onecan see that the edge detection operators can be calculated by spatial gradient from $\hat{s}$ as follows.

$$\nabla\{\hat{s}\} = \nabla\{\hat{s}_{ML}\} + \nabla\{\beta_\alpha[x - \alpha.\hat{s}_{ML}]\} = \beta_\alpha\nabla\{x\} + x\nabla\{\beta_\alpha\} + \nabla\{\hat{s}_{ML}\} - \nabla\{\alpha.\beta_\alpha.\hat{s}_{ML}\} \quad (25)$$

Well-known edge detection operators such as Sobel, Prewitt and Canny can be used for $\nabla\{x\} = \nabla\{x_r\} + \nabla\{x_i\}$ [11, 19]. The indices (r), and (i) point to the real and imaginary parts of the impedance variations which is mapped as two dimensional C-Scan Images.

As seen in (25), the linear spatial gradient of the noisy image $(x), \nabla\{x\}$, is multiplied by β_α. Also, (24) confirms that the value of β_α is obtained for a minimum error. Thus, we can heuristically expect that the boundary detection operator is sharpened when using a weighting factor.

5. Results

To examine the validity of the proposed method, several simulated and experimental tests were carried out. For brevity, we present the results associated with a simulated circular object and a semi-circular hole in an iron block.

A. Simulated Results

To study the simulated results, a simulated circular object with gradient changes on its intensity is used. Fig (2-a) shows the original object and the image shown in Fig (2-b) is obtained by addition of Gaussian noise. The results of three methods, *i.e.,* the Wiener, SAML and MSAML filters are compared with three sizes of local windows (W=3*3, 5*5, and 9*9). Increasing the size of local window in the Wiener filter results in blurring the edges of the object and eliminating the details, as shown in Figs (3-a, b and c). Using the SAML filter, a better contrast is achieved; however, increasing the size of the local window (e.g., W=9*9) causes blurring in the edges of the recognized object. The results of the SAML filter are shown in Figs. 4 (a), (b), and (c). Figs. 4 (d), (e) and (f) show the results of the weighting factor β that correspond to the enhancement of the object boundary. Figs. 5 (a), (b) and (c) show the results of the noise removal for the MSAML filter and Figs. 6 (d), (e) and (f) shows the boundary detection enhancement for the object which is obtained from weighting factor $\beta_{\max}$.

Figs. 6 (a), and (b) show the results of error between the original and the filtered noisy image when the Wiener, SAML and MSAML filters are used, respectively. From Figs (4-6), it is seen that the results of the MSAML and SAML filters are better than the corresponding results of the Wiener filter. Also, the most successful results for boundary detection are obtained from the MSAML filter. Furthermore, The MSAML filter, in addition to better contrast in object detection, has better sharpness relative to the corresponding results of the Wiener and SAML filters.

B. Experimental Results

The proposed image enhancing methods are applied to a C-scan image from inspecting defect on the iron surface area, using the eddy current technique. The surface of the sample has porosity which, in turn, makes it difficult detect surface defects. Figs. 7 (a), and (b) are C-Scan images of real and imaginary parts of an impedance variation of the absolute EC probe with frequency 100 KHz. Fig. 7 (c) also shows the absolute impedance variation of the probe. The complex values of mean and variance of these images are, respectively, estimated to

be $\mu_r = 0.2093$, $\sigma_r = 0.0549$, $\mu_i = 0.1930$, $\sigma_i = 0.0802$.

We first compare the noise suppression results of the AML (Figs. 7 (g), (h) and (i)) and MAML (Figs. 7 (j), (i) and (k)) filters with those obtained using the Wiener filter, Figs. 7 (d), (e) and (f). A comparison of the results shown in Fig 8 demonstrates that the AML and MAML filters are more appealing over the Wiener filter for noise filtration.

Next, we compare the defect detection capability of various filters. Figs. 8 (a), and (b) and 8 (c), and (d) show, respectively, the results of AML and MAML edge enhancement for the real and imaginary parts of the C-Scan images given in Figs. 7 (a), and (b). These results show that the MAML boundary detection operator performs more effectively in detection of details (such as porosity) relative to its AML counterpart.

6. CONCLUSION

A nonlinear adaptive filter based on maximum likelihood criterion (AML) is designed for defect detection in EC inspection of materials. The model of EC noise in this filter is assumed to be non-zero mean complex Gaussian process. The AML filter is modified by an enhancing factor for better detection of defect details. Also, an edge detection operator is introduced for boundary detection of defects. This method is successful when the signal energy is larger than the variance of noise. Otherwise, the maximum likelihood estimation is found to be more efficient. Simulated and experimental results demonstrate that both the AML and MAML filters are superior over their rival Wiener filter. In addition, the MAML boundary detection operator is found to be more effective in detection of details of a defect as compared to its corresponding AML counterpart.

7. REFERENCES

[1] Bray DE, McBride D., "Nondestructive testing techniques", New York: John Wiley & Sons, Inc, 1992.

[2] Dogandzic A., Xiang P., "Estimation statistical properties of eddy current signals from steam generator tubes", IEEE Trans. Signal Processing, vol. 53, no 8, pp.3342-3348, 2005.

[3] Groshong B. R., Bilbro G. L., Synder W. E., "Eddy current restoration by constrained gradient", Journal of Nondestructive Evaluation, vol. 10, no 4, 1991.

[4] Kotropoulos C. et al, "Nonlinear ultrasonic image processing based on signal-adaptive filters and self-organizing neural networks", IEEE Trans. Image Processing, vol. 3, no. 1, pp. 65-77, 1994.

[5] Macovski A., "Noise in MRI", Magn. Reson. Med., vol. 36, no 3, pp., 494-497, 1996.

[6] Kuan D.T., Sawchuk A. A., Strand T. C., Chavel P., "Adaptive noise smoothing filter for images with signal-dependent noise", IEEE Trans., Pattern Anal. Mach. Intell. Vol. PAMI-7, no 2, pp. 165-177, 1985.

[7] Pitas I., Venetsanopoulos A. N., "Nonlinear mean filters in image processing", IEEE Trans Acoustic, Speech and Signal Processing, vol. ASSP-34, no 3, 1986.

[8] Mitra S. K., Sicuranza G. L., "Nonlinear image processing", Academic Press, 2001.

[9] Wrzuszczak M., Wrzuszczak J., "Eddy current flaw detection with neural network applications", Measurement, vol. 38, pp. 132-136, 2005.

[10] Sarkar S., Boyer K. L., "On optimal infinite impulse response edge detection filters", IEEE Trans on Pattern Analysis & Machine Intelligence, vol. 13, no 11, 1991.

[11] Bovik A., "Handbook of Image and Video Processing", Academic Press, 2000.

[12] Bernstein R., "Adaptive nonlinear filters for simulations removal of different kinds of noise in images", IEEE Trans. Circuit Syst., vol. CAS-34, no 11, pp. 1275-1291, 1987.

[13] Pitas I., Venetsanopoulos A. N., "Nonlinear digital filters: Principles and Applications", Hingham, MA: Kluwer, 1990.

[14] Aldrin J. C., Knopp J. S., "Crack characterization method with invariance to noise features for eddy current inspection of fastener sites", Journal of Nondestructive Evaluation vol. 25, no 4, 2006.

[15] Fukunaga K, "Introduction to statistical pattern recognition", Academic Press, 1990.

[16] Huang H., Takagi T., Fukutomi H., "Fast signal predictions of noised signals in eddy current testing", IEEE Trans. Magnetics, vol. 36, no 4, pp. 1719-1723, 2000.

[17] Chen G., Yamaguchi A., Miya K., "A novel signal processing technique for eddy-current testing of steam generator tubes", IEEE Trans Magnetics, vol. 34, no 3, 1998.

[18] Hasanzadeh P.R. R., Rezaie A.H., Sadeghi S.H.H., Moradi M.H., Ahmadi M., "A density based fuzzy clustering technique for non-destructive detection of defects in materials", NDT&E International, vol. 40, no 4, pp. 337-346, 2007.

[19] Hasanzadeh P.R.R., "Defect detection in metallic structures by EC method using a combined image processing and fuzzy logic techniques", PhD Dissertation, Elect. Eng. Dept., Amirkabir University of Technology, September 2007.

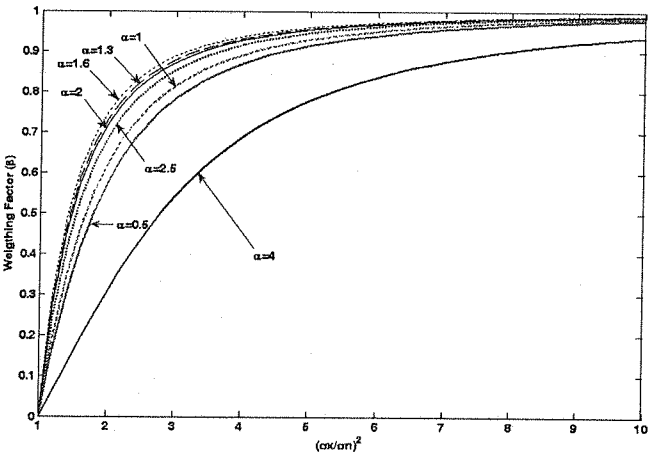

Fig 1. Variation of weighting factor β versus $(\frac{\sigma_x}{\sigma_n})^2$ for different values of scaling factor α when $\sigma_n = 1$, $\mu = 0.6$ and $\hat{s}_{ML} = 1$ ($\alpha_{\beta_{\max}} = 1.6$).

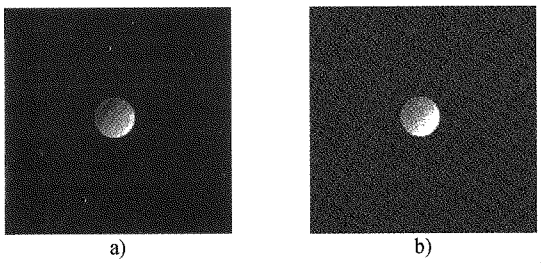

a) b)

Fig 2. Simulated images of a circular object in noise-free and noisy conditions. a) Original Image, b) Real Gaussian noise with μ=0.2 and σ_n=0.005 is added

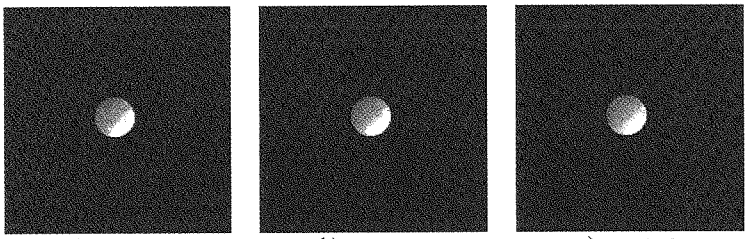

a) $W = 3\times3$ b) $W = 5\times5$ c) $W = 9\times9$

Fig 3. Reconstructed images of the circular object shown in Fig. 3(b) when using the Wiener filter with different local window sizes.

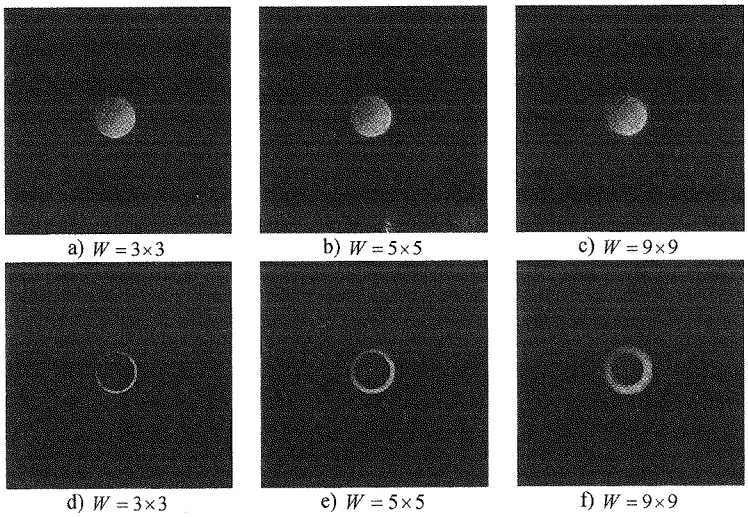

a) $W = 3\times3$ b) $W = 5\times5$ c) $W = 9\times9$

d) $W = 3\times3$ e) $W = 5\times5$ f) $W = 9\times9$

Figs. 4 (a), (b) and (c), Reconstructed images of the circular object shown in Fig. 3(b) when using the AML filter with different local window sizes; (d), (e), and (f) Their respective weighting factor (β) images.

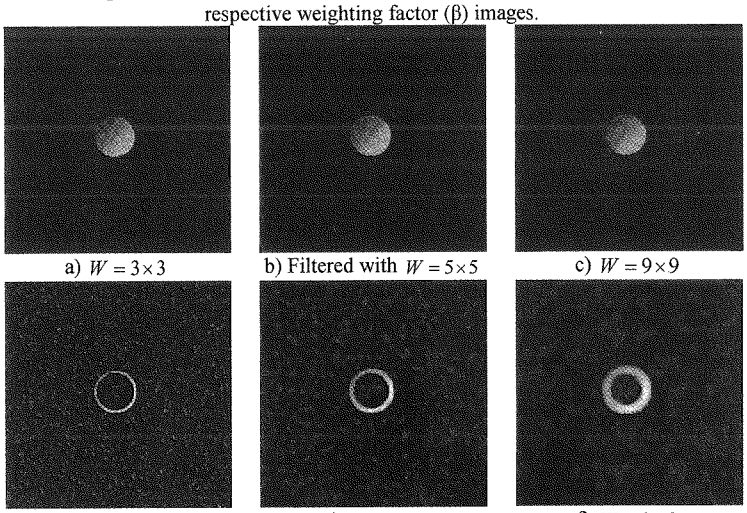

a) $W = 3\times3$ b) Filtered with $W = 5\times5$ c) $W = 9\times9$

d) $W = 3\times3$ e) $W = 5\times5$ f) $W = 9\times9$

Fig. 5 (a), (b) and (c). Reconstructed images of the circular object shown in Fig. 3(b) when using the MAML filter with different local window sizes; (d), (e), and (f) Their respective weighting factor (β) images.

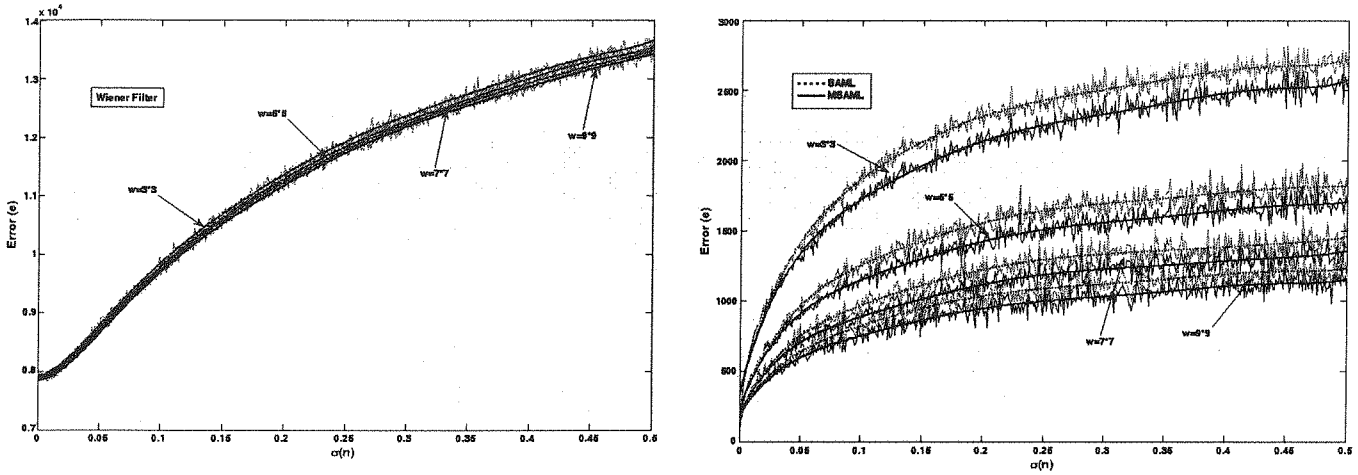

a) Wiener Filter b) SAML and MSAML Filter

Fig 6. Errors between the original circular object (Fig. 3a) and its reconstructed image versus noise variance when using (a) the Wiener and (b) the AML and MAML filters. Results are obtained and compared for window sizes of 3×3 , 5×5 , 7×7 and 9×9 .

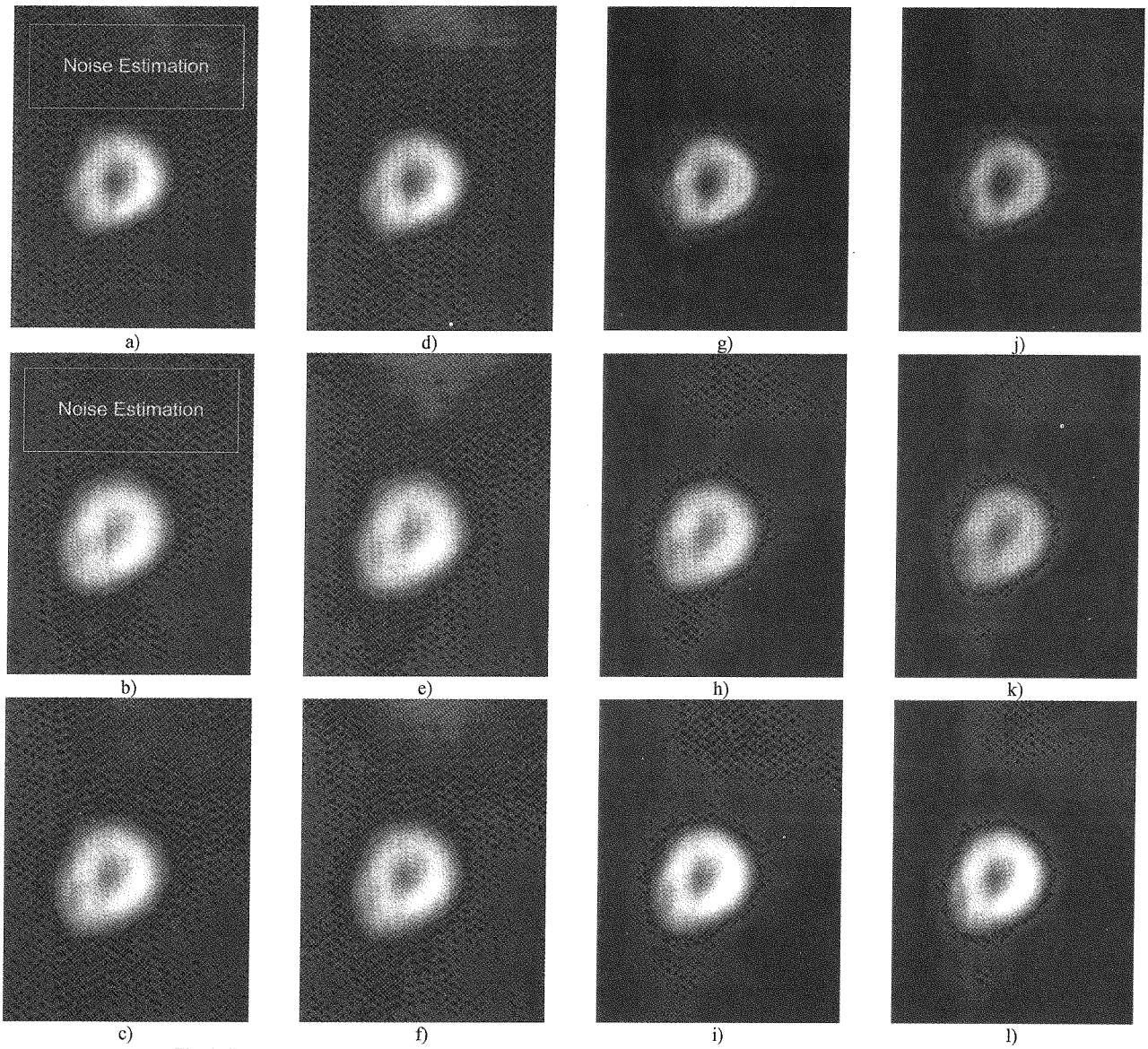

a) d) g) j)

b) e) h) k)

c) f) i) l)

Fig. 7, Reconstructed images of a surface inclusion in a mild steel specimen using its C-scan EC data.
(a) Real, (b) imaginary, and (c) magnitude of the original data and their respective Wiener filter (d), (e), and (f), AML filter (g), (h), and (i), and MAML filter reconstructed images when using a window size $W = 5\times5$.

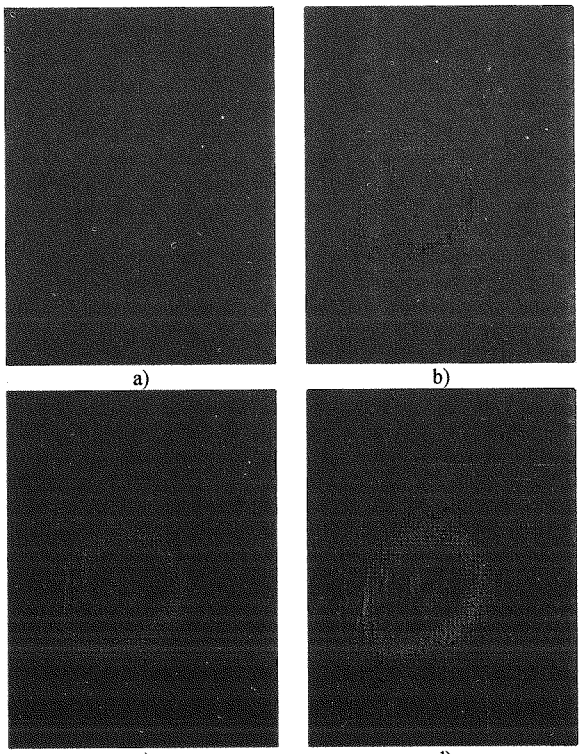

Fig 8. Enhancing factor of the boundary detection operator when using the (a, b) AML and (c, d) MAML filters for a window size of $W = 5 \times 5$. (a) and c) are real parts and b) and d) are imaginary parts.)

Table 1: Signal estimation models and their weighting factors.

	Signal Estimation		Weighting Factor
	$\sigma_x \geq \sigma_n$	$\sigma_x < \sigma_n$	
General Form	$\hat{s} = \hat{s}_{ML} + \beta_\alpha.[x - \alpha\hat{s}_{ML}]$	$\hat{s} = \hat{s}_{ML}$	$\beta_\alpha = 1 - \frac{(\sigma_n^2 + [\mu - (\alpha-1).\hat{s}_{ML}]^2)}{(\sigma_x^2 + [\mu - (\alpha-1).\hat{s}_{ML}]^2)}$
AML ($\alpha=1$)	$\hat{s} = \hat{s}_{ML} + \beta.[x - \hat{s}_{ML}]$	$\hat{s} = \hat{s}_{ML}$	$\beta = 1 - (\frac{\sigma_n^2 + \mu^2}{\sigma_x^2 + \mu^2})$
MAML	$\hat{s} = (1 - \beta_{\max}).\hat{s}_{ML} + \beta_{\max}.[x - \mu]$	$\hat{s} = \hat{s}_{ML}$	$\beta = 1 - (\frac{\sigma_n}{\sigma_x})^2$